

# Extreme Ultraviolet Lithography Capabilities at the Advanced Light Source Using a 0.3-NA Optic

Patrick Naulleau, Kenneth A. Goldberg, Jason P. Cain, Erik H. Anderson, Kim R. Dean, Paul Denham, Brian Hoef, and Keith H. Jackson

**Abstract**—Extreme ultraviolet lithography is a leading candidate for volume production of nanoelectronics at the 32-nm node and beyond. In order to ensure adequate maturity of the technology by the start date for the 32-nm node, advanced development tools are required today with numerical apertures of 0.25 or larger. In order to meet these development needs, a microexposure tool based on SEMATECH's 0.3-numerical aperture microfield optic has been developed and implemented at Lawrence Berkeley National Laboratory, Berkeley, CA.

Here we describe the Berkeley exposure tool in detail, discuss its characterization, and summarize printing results obtained over the past year. Limited by the availability of ultrahigh resolution chemically amplified resists, present resolving capabilities limits are approximately 32 nm for equal lines and spaces and 28 nm for semi-isolated lines.

**Index Terms**—Extreme ultraviolet (EUV), lithography.

## I. INTRODUCTION

FOR volume nanoelectronics production using extreme ultraviolet (EUV) lithography [1] to become a reality around the year 2011, advanced EUV research tools are required today. Microfield exposure tools have played a vital role in the early development of EUV lithography [2]–[4] concentrating on numerical apertures (NA) of 0.2 and smaller. Expected to enter production at the 32-nm node with numerical apertures (NAs) of 0.25, however, EUV can no longer rely on these early research tools to provide relevant learning. To overcome this problem, a new generation of microfield exposure tools, operating at an NA of 0.3 have been developed [5]–[8]. Like their predecessors, these tools tradeoff field size and speed for greatly reduced complexity.

Source development remains a significant issue for EUV lithography. However, a majority of the issues crucial to source

Manuscript received June 10, 2005; revised July 22, 2005. This work was performed at Lawrence Berkeley National Laboratory, Berkeley, CA, and supported in part by SEMATECH. Lawrence Berkeley National Laboratory is operated under the auspices of the Director, Office of Science, Office of Basic Energy Science, of the U.S. Department of Energy.

P. Naulleau is with the College of Nanoscale Science and Engineering, University at Albany, Albany, NY 12203 USA (e-mail: PNaulleau@uamail.albany.edu).

K. A. Goldberg, E. H. Anderson, P. Denham, B. Hoef, and K. H. Jackson are with the Center for X-Ray Optics, Lawrence Berkeley National Laboratory, Berkeley, CA 94720 USA (e-mail: KAGoldberg@lbl.gov; EHanderson@lbl.gov; PEDenham@lbl.gov; BHHoef@lbl.gov; KH-jackson@lbl.gov).

J. P. Cain is with AMD, Sunnyvale, CA 94088 USA (e-mail: jason.cain@amd.com).

K. R. Dean is with SEMATECH, Austin, TX 78741 USA (e-mail: Kim.Dean@sematech.org).

Digital Object Identifier 10.1109/JQE.2005.858450

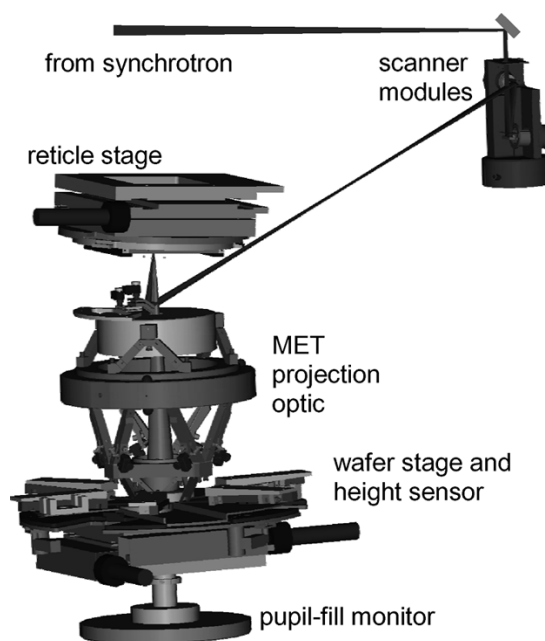


Fig. 1. Model depicting the major exposure station components and the EUV beam path (the system is described in detail in [5]).

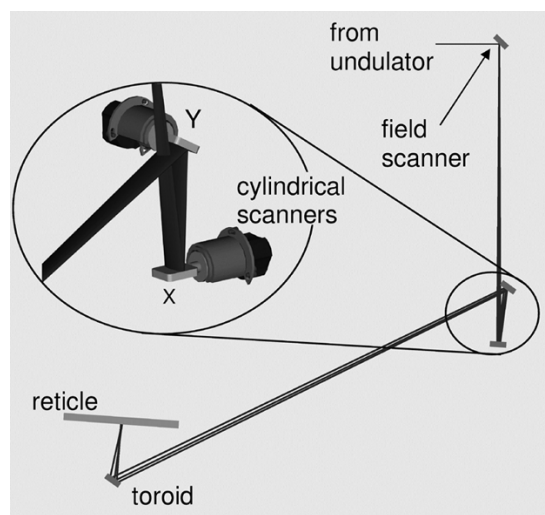


Fig. 2. Schematic of the MET programmable coherence illuminator. The pupil scanner mirrors are both cylindrical with power in the scanning direction. In addition to the pupil scanners, the illuminator includes a two-dimensional field uniformity scanner.

development can be studied separately from a functional exposure tool, thus the design of developmental EUV lithography systems can be further simplified through the use of

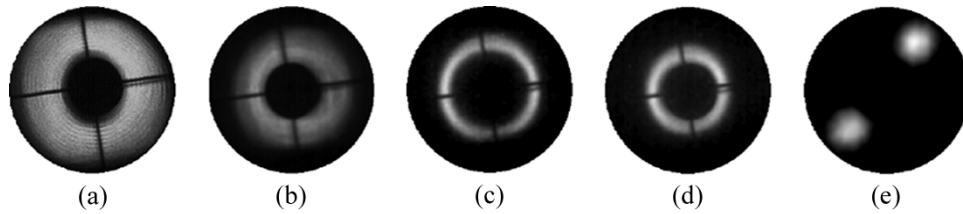


Fig. 3. EUV pupil fills recorded through the MET exposure system using the *in situ* pupil-fill monitor. The illuminator can access a  $\sigma$  range of up to 1.2 in  $x$  and 0.8 in  $y$ . (a) Annular fill  $0.3 < \sigma < 0.9$ . (b) Annular fill  $0.3 < \sigma < 0.7$ . (c) Annular fill  $0.45 < \sigma < 0.55$ . (d) Annular fill  $0.35 < \sigma < 0.45$ . (e)  $45^\circ$  oriented dipole.

synchrotron sources. Although clearly not viable solutions for volume production, these well characterized, spectrally pure, debris free, and reliable sources are an excellent choice for microfield research tools. It is important to note, however, that the intrinsic coherence properties of synchrotron radiation [9], [10] are a poor match for lithography applications, yet this potential problem can readily be dealt with using an active illuminator scheme [11]. This approach has the added benefit of enabling the implementation of a high efficiency programmable coherence (pupil fill) illuminator.

Here we describe the Berkeley exposure tool in detail, discuss its characterization, and summarize printing results obtained over the past year. Limited by the availability of ultrahigh resolution chemically amplified resists, present resolving capabilities are approximately 32 nm for equal lines and spaces and 28 nm for semi-isolated lines.

## II. SYSTEM CONFIGURATION

The EUV microfield exposure tool is implemented at Lawrence Berkeley National Laboratory's Advanced Light Source synchrotron radiation facility. It utilizes SEMATECH's  $5\times$ -reduction, 0.3-NA Micro-Exposure Tool (MET) optic [12], [13]. The MET optic has a well-corrected field of view of  $1 \times 3$  mm at the reticle plane ( $200 \times 600 \mu\text{m}$  at the wafer plane). The computer-aided design (CAD) model shown in Fig. 1 depicts the major exposure station components as well as the EUV beam path (the system is described in detail in [5]). Effectively coherent radiation from an undulator beamline [9], [10] at the advanced light source impinges on the scanning illuminator. The light is directed to a reflective reticle mounted at an angle of  $4^\circ$ . From there the light is re-imaged by the MET optic with  $5\times$  demagnification to the tilted wafer plane. A grazing incidence laser system is used to monitor the height of the wafer at the print site ensuring that it remains in focus [14]. With the wafer removed, the light propagates to a scintillator plate sitting effectively in the far field. Pupil-fill monitoring is achieved by re-imaging the scintillator plate through a vacuum window to a visible-light charge-coupled device (CCD) camera.

The illuminator used in the MET exposure station (Fig. 2) is based on a scanning Fourier synthesis scheme allowing arbitrary coherence functions to be generated [11]. The illuminator is designed to support the large NA of the MET optic as well as its full field of view and short exposure times [15]. The pupil scanning capabilities are provided by two one-dimensional vacuum compatible flexure suspension galvanometers<sup>1</sup> enabling exposure times as short as 30-ms for certain pupil fills.

<sup>1</sup>The flexure suspension galvanometers were manufactured by Nutfield Technology Inc., 49 Range Road, Windham, NH 03087 USA.

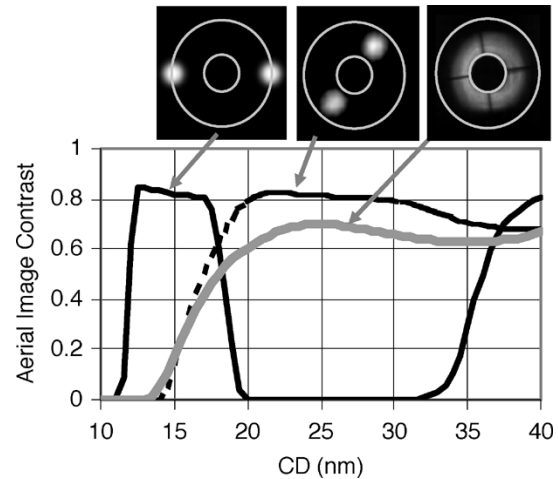


Fig. 4. Modeling of the aerial image contrast transfer function for three different pupil fills.

Both scanning mirrors are cylindrical with power in the scanning direction. They are designed to focus the incoming undulator radiation to the front focal plane of the toroidal condensor mirror, which itself is used to re-image the scanners to the reticle. This configuration provides for illumination stationarity across the  $200 \times 600 \mu\text{m}$  field of view [15]. In addition to the pupil scanners, the MET illuminator also includes a field uniformity scanner comprised of a flat mirror. This scanning mirror is used to improve the short-range uniformity of the illumination but is not intended to synthesize the illumination field size.

Fig. 3 shows a series of EUV pupil fills recorded using the pupil fill monitor. In the large annular ( $0.35 < \sigma < 0.85$ ) illumination case, we see the onset of vignetting in the  $y$  direction as evidenced by the squaring off of the pupil fill. This effect is due to the limited extent of the toroid in the  $y$  direction. The size of the toroid was constrained to prevent obscuration of imaging rays leaving the reticle and entering the MET optic. This limitation does not exist in the  $x$  direction, where the toroid supports  $\sigma > 1$ . In the pupil-fill monitor images we also see the MET central obscuration as well as the arms used to support the direct-transmission-blocking baffles.

## III. PREDICTED RESOLUTION LIMIT

With a NA of 0.3, the MET optic has a Rayleigh resolution ( $k_1$  factor = 0.61) of 27 nm. As shown in Fig. 4, using a programmable coherence illuminator, however, enables the  $k_1$  factor to be pushed significantly below the Rayleigh limit. The EUV measured wavefront [16], [17] is used in the modeling of all cases shown in Fig. 4. Under standard annular illumination ( $0.3 < \sigma < 0.7$ ) the resolution knee occurs at about 23 nm.

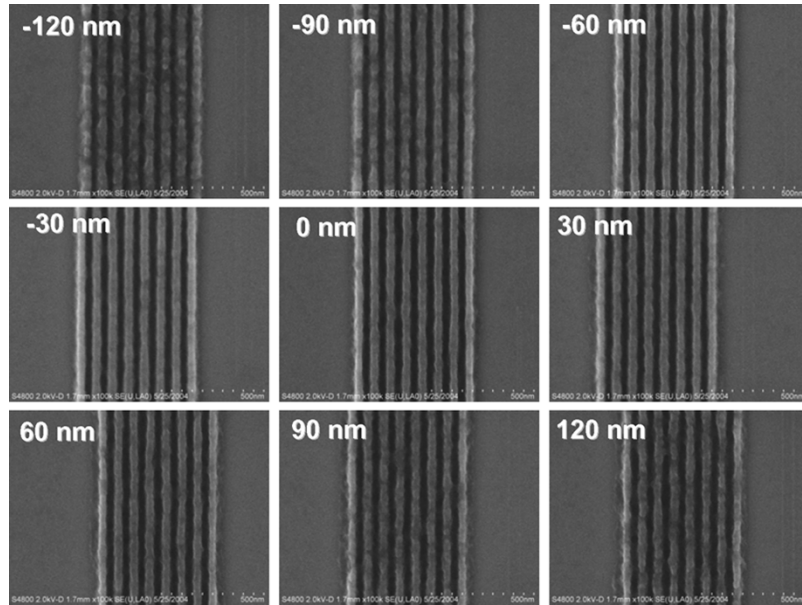


Fig. 5. Through-focus (30-nm steps) series of 40-nm lines and spaces in *MET-1K* resist under annular illumination.

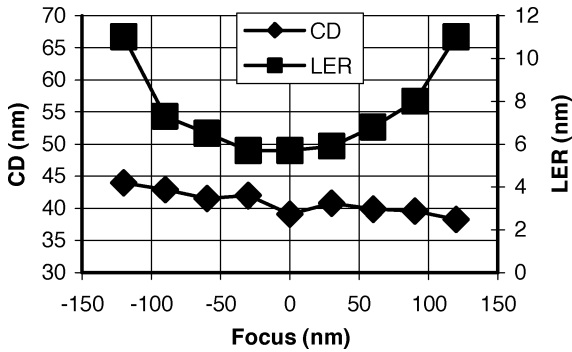


Fig. 6. Plot of the measured LER and feature size through focus for the through-focus images in Fig. 4. The smooth behavior of the through-focus data is an indication of the good focus control performance.

Going to 45-degree dipole illumination, the resolution knee is pushed out to approximately 20 nm and the aerial-image contrast generally enhanced. Ultimate resolution on vertical lines can be achieved by going to  $x$ -dipole illumination with an offset  $\sigma$  of 1, in which case the resolution knee is pushed down to 12.5 nm.

As a result of the interaction between the diffracted orders from the mask and the central obscuration of the MET optic, the  $x$ -dipole illumination shows a contrast dead band in the 20–35-nm range. Moreover, the  $x$ -dipole case can be shown to suffer from very poor performance on horizontal features. Both these problems can be overcome by using the 45° dipole condition while still achieving a resolution knee of 20 nm, considerably better than any currently available chemically amplified resist.

#### IV. TOOL CHARACTERIZATION

Because the above-described tool is intended, in large part, for use in the development of EUV resist and mask processes, it is important to characterize the system performance and stability. For this task we choose to use one of the best performing

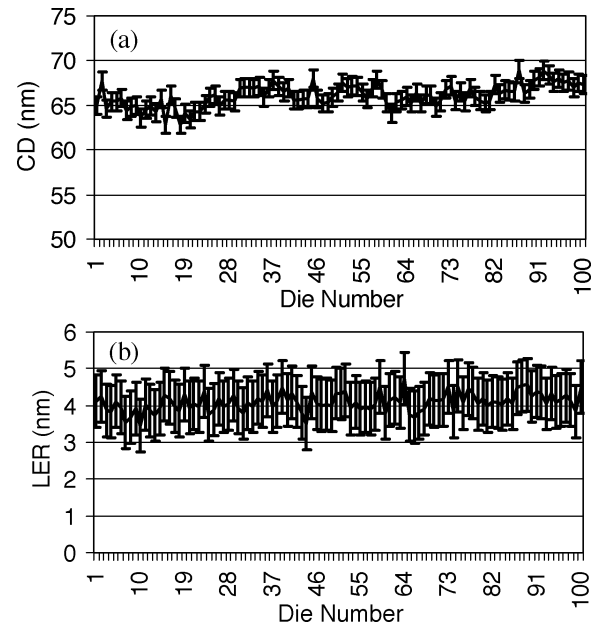


Fig. 7. Die-to-die reproducibility of (a) CD and (b) LER on 60-nm coded lines and spaces printed in *MET-1K* resist.

EUV resists tested to date: Rohm and Haas *MET-1K* resist (XP3454C). This resist has been extensively characterized and reported on [6], [18], [19] over the past year and has been shown to have significantly better resolution than the previous generation of EUV resists such as Rohm and Haas *EUV-2D*.

Performing relevant lithographic characterization requires the ability to actuate focus to a fraction of the nominally 100-nm depth of focus. Figs. 5 and 6 demonstrate the Berkeley tool focus-control capabilities by showing a series of 40-nm lines and space images through focus in 30-nm steps under annular ( $0.3 < \sigma < 0.7$ ) illumination. The stable focus control is evident in the images themselves (Fig. 5) as well as in the extracted line-edge roughness (LER) and critical dimension (CD) data (Fig. 6).

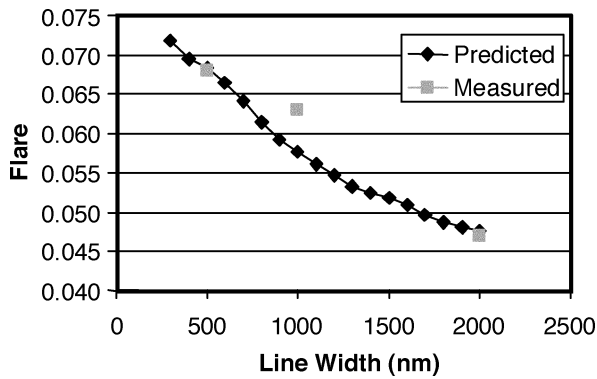


Fig. 8. Direct comparison of measured and predicted flare in the MET optic. Lithographic measurement performed using the Kirk method.

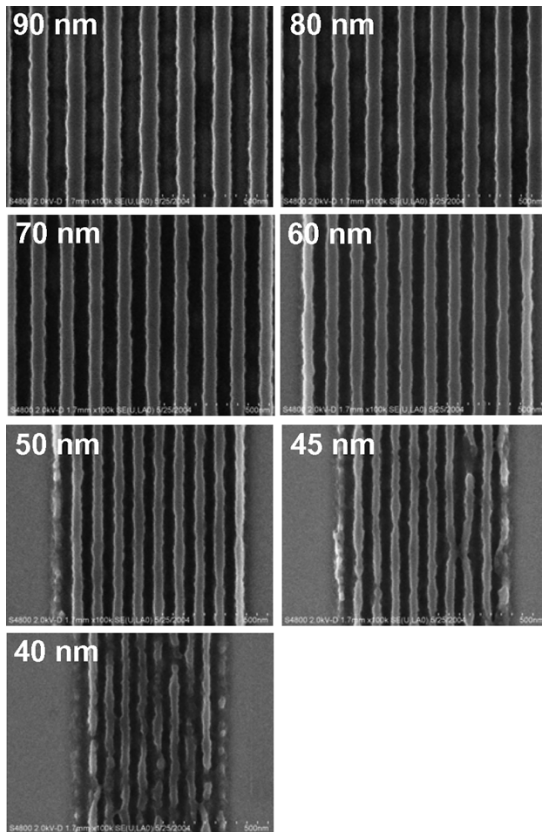


Fig. 9. Equal lines and spaces printed in 125-nm-thick layer of Rohm and Haas EUV-2D resist. The pupil fill was annular 0.3–0.7.

To explicitly evaluate tool stability, we examine die-to-die performance. Fig. 7 shows CD and LER results from 60-nm line-space features in 100 identically exposed die (same dose and focus) on a single wafer. The error bars on the CD data correspond to the variation observed from repeated measurements of the same die as well as line-to-line variations within a single image. The measured die-to-die rms CD variation is 1.2 nm; based on the previously measured CD sensitivity to dose, this CD variation corresponds to a rms dose variation of 1.5%. Fig. 7(b) shows the LER die-to-die variation to be significantly smaller than the observed line-to-line LER variation depicted by the error bars, again indicating stable tool performance.

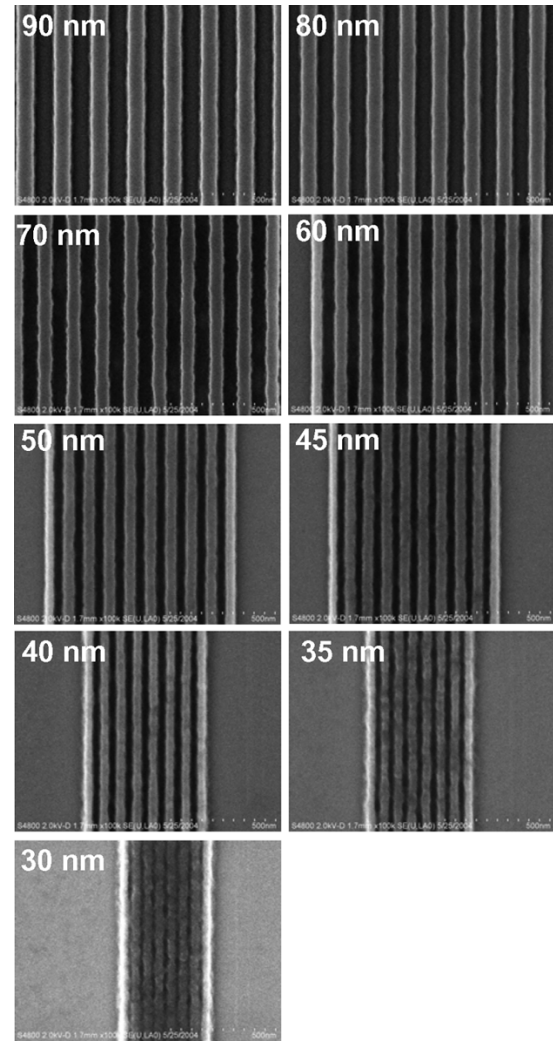


Fig. 10. Equal lines and spaces printed in 125-nm-thick layer of Rohm and Haas MET-1K resist. As in Fig. 9, the pupil fill was annular 0.3–0.7.

Owing to the extremely short wavelength and reflective nature of EUV optics, scatter, and thus flare, is a significant concern. Flare in the MET optic has been predicted to be quite low based on surface metrology of the individual optics, however, the flare was never directly measured in the assembled system using scatterometry techniques. To verify the predicted flare values, it is thus important to perform a lithographic measurement. Although MET-1K is well suited for high-resolution work as described above, its relatively low cross-linking threshold makes it unsuitable for characterization of flare. Not requiring high-resolution printing, flare tests can be implemented using Rohm and Haas EUV-2D resist. Fig. 8 shows a direct comparison of the predicted and measured flare as a function of feature size, validating the predicted value of 7% flare in a 500-nm line within a  $200 \times 600 - \mu\text{m}$  field. A more detailed description of the flare measurement can be found in the literature [20].

## V. RESIST CHARACTERIZATION

Since printing operations began in February 2004, more than 140 resist and 12 masks have been tested by users from 15 different organizations. The system has already played a crucial

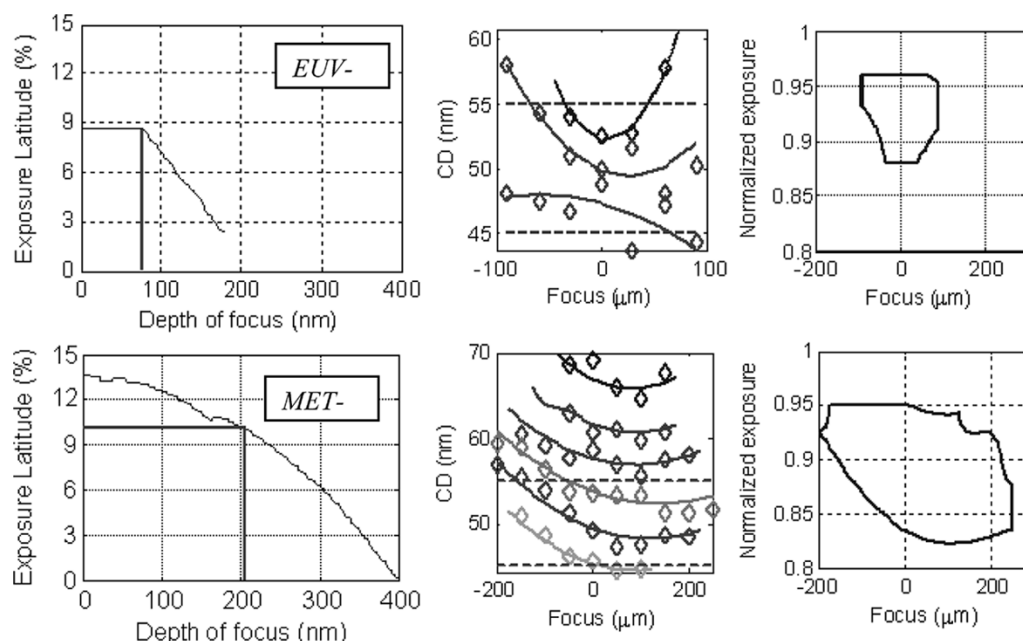


Fig. 11. Direct process window comparison on 50-nm lines space features between *EUV-2D* and *MET-1K* resist. The exposure conditions are as described in Figs. 9 and 10. The process window constraints are set to  $\pm 10\%$  CD change. The Bossung curves are based on 5% dose steps.

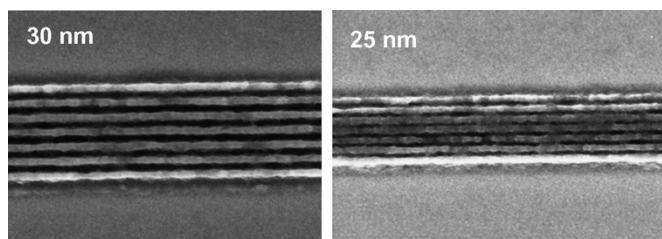


Fig. 12. Printing of 30- and 25-nm equal lines and spaces in *MET-1K* resist using monopole illumination.

role in enabling the development of high-resolution chemically amplified resists. In the past, the mainstay resist of EUV research in the US was Rohm and Haas *EUV-2D*, however, this resist has now been shown (Fig. 9) to have a resolution limit of approximately 45 nm, in good agreement with previous predictions [21], [22].

With high-resolution printing feedback, resist-based limitations could easily be observed, enabling superior formulations to be identified. Using this method, the above-described *MET-1K* resist was selected as one of the best performers. The *MET-1K* printing results in Fig. 10 show that the optic is capable of at least 30-nm printing. Moreover, these results serve to verify the assertion that the printing limits observed in Fig. 9 are indeed due to the resist, and not the aerial-image.

A more quantitative comparison of *EUV-2D* and *MET-1K* can be achieved through process window analysis. Fig. 11 shows the direct *EUV-2D* to *MET-1K* process window comparison for 50-nm features (the Bossung curves are based on 5% dose steps). In *EUV-2D* the depth of focus is only 90 nm at an exposure latitude limit of below 9%, whereas *MET-1K* displays a depth of focus of 200 nm at an exposure latitude of 10%. In all cases, the process window size is based on  $\pm 10\%$  CD change.

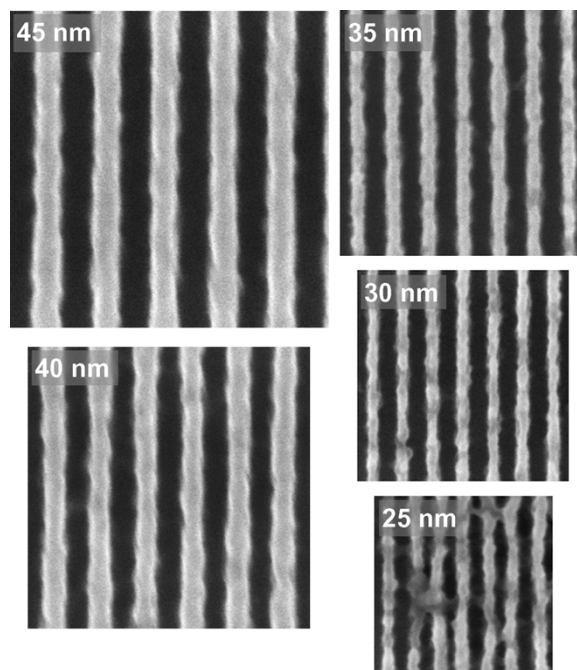


Fig. 13. Equal line space images ranging from 45 to 25 nm printed in experimental *KRS* resist under annular illumination  $0.3 < \sigma < 0.7$ . Contrary to the results in Fig. 4, which show the aerial-image contrast to improve as the feature size goes from 35 to 25 nm, it is evident that the imaging performance degrades rapidly for sizes below 35 nm. These results again indicate resist limited performance as opposed to an aerial-image limit.

Based on Fig. 4, one might expect the performance of *MET-1K* to improve slightly by employing dipole, or its near equivalent, monopole, illumination. Fig. 12 shows prints of 30-nm and 25-nm equal lines and spaces printed in *MET-1K* under monopole illumination. The pole-offset radius was 0.6 at  $45^\circ$  and the pole radius was 0.2. A slight improvement is seen,

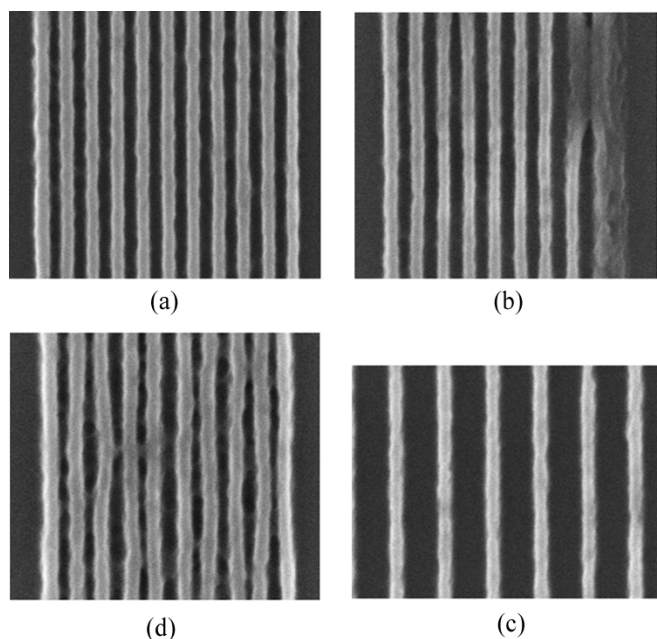


Fig. 14. Images recorded in *KRS* resist under  $\gamma$ -monopole illumination. (a) 35-nm lines and spaces. (b) 32.5-nm lines and spaces. (c) 30-nm lines and spaces. (d) Coded 27.5-nm lines 110-nm pitch, actual printed size in resist is 28.3-nm.

however, the 30-nm resolution cutoff is still evident suggesting that the limit is indeed resist induced.

Of the greater than 140 resists tested in the Berkeley system, there have been two groups of clear stand-outs: one of these groups is *MET-1K* and its variants and the other group is experimental *KRS* resists provided by IBM [23]. Fig. 13 shows a series of equal line space images ranging from 45 to 25 nm printed in experimental *KRS* resist under annular illumination ( $0.3 < \sigma < 0.7$ ). Contrary to the results in Fig. 4, which show the aerial-image contrast to improve as the feature size goes from 35 to 25 nm, it is evident that the imaging performance degrades rapidly for sizes below 35 nm. These results again indicate resist limited performance as opposed to an aerial-image limit.

Fig. 14 shows a series of images recorded in *KRS* resist under monopole illumination. Consistent with resist-limited performance, the monopole illumination has its greatest effect on feature sizes greater than 30 nm. Monopole illumination, however, does also enable the printing of sub-30-nm semi-isolated features as shown in Fig. 14(d).

## VI. SUMMARY

The 0.3-NA Berkeley exposure tool utilizing synchrotron illumination and a programmable coherence illuminator has been described. Detailed characterization of the exposure tool indicates that the system is operating to specification. Printing results further indicate that EUV performance is presently resist limited. The best resolving resist tested to date is capable of approximately 32-nm nested resolution and 28-nm isolated line resolution.

## ACKNOWLEDGMENT

The authors would like to thank R. Brainard and T. Koehler of Rohm and Haas as well as G. Wallraff and C. Larson of IBM for providing resist materials and expert processing support. They also acknowledge the entire CXRO staff for enabling this research.

## REFERENCES

- [1] R. Stulen and D. Sweeney, "Extreme ultraviolet lithography," *IEEE J. Quantum Electron.*, vol. 35, no. 5, pp. 694–699, May 1999.
- [2] J. Goldsmith, K. Berger, D. Bozman, G. Cardinale, D. Folk, C. Henderson, D. O'Connell, A. Ray-Chaudhuri, K. Stewart, D. Tichenor, H. Chapman, R. Gaughan, R. Hudyma, C. Montcalm, E. Spiller, J. Taylor, J. Williams, K. Goldberg, E. Gullikson, P. Naulleau, and J. Cobb, "Sub-100-nm lithographic imaging with an EUV 10' microstepper," *Proc. SPIE*, vol. 3676, pp. 264–271, 1999.
- [3] K. Hamamoto, T. Watanabe, H. Tsubakino, H. Kinoshita, T. Shoki, and M. Hosoya, "Fine pattern replication by EUV lithography," *J. Photopolymer Sci. Technol.*, vol. 14, pp. 567–572, 2001.
- [4] P. Naulleau, K. Goldberg, E. Anderson, D. Attwood, P. Batson, J. Bokor, P. Denham, E. Gullikson, B. Harteneck, B. Hoef, K. Jackson, D. Olynick, S. Rekawa, F. Salmassi, K. Blaedel, H. Chapman, L. Hale, P. Mirkarimi, R. Soufli, E. Spiller, D. Sweeney, J. Taylor, C. Walton, D. O'Connell, R. Stulen, D. Tichenor, C. Gwyn, P. Yan, and G. Zhang, "Sub-70 nm extreme ultraviolet lithography at the advanced light source static microfield exposure station using the engineering test stand set-2 optic," *J. Vac. Sci. Technol.*, vol. B 20, pp. 2829–2833, 2002.
- [5] P. Naulleau, K. Goldberg, E. Anderson, K. Bradley, R. Delano, P. Denham, R. Gunion, B. Harteneck, B. Hoef, H. Huang, K. Jackson, M. Jones, D. Kemp, J. Liddle, R. Oort, A. Rawlins, S. Rekawa, F. Salmassi, R. Tackaberry, C. Chung, L. Hale, D. Phillion, G. Sommargren, and H. Taylor, "Status of EUV micro-exposure capabilities at the ALS using the 0.3-NA MET optic," *Proc. SPIE*, vol. 5374, pp. 881–891, 2004.
- [6] P. Naulleau, K. Goldberg, E. Anderson, J. Cain, P. Denham, K. Jackson, A. Morlens, S. Rekawa, and F. Salmassi, "Extreme ultraviolet microexposures at the Advanced Light Source using the 0.3 numerical aperture micro-exposure tool optic," *J. Vac. Sci. Technol.*, vol. B 22, pp. 2962–2965, 2004.
- [7] A. Brunton, J. S. Cashmore, P. Elbourn, G. Elliner, M. C. Gower, P. Gruenewald, M. Harman, S. Hough, N. McEntee, S. Mundair, D. Rees, P. Richards, V. Truffert, I. Wallhead, and M. D. Whitfield, "High-resolution EUV imaging tools for resist exposure and aerial image monitoring," *Proc. SPIE*, vol. 5751, pp. 78–89, 2005.
- [8] H. Oizumi, Y. Tanaka, I. Nishiyama, H. Kondo, and K. Murakami, "Lithographic performance of high-numerical-aperture ( $NA = 0.3$ ) EUV small-field exposure tool (HINA)," *Proc. SPIE*, vol. 5751, pp. 102–109, 2005.
- [9] D. Attwood, G. Sommargren, R. Beguiristain, K. Nguyen, J. Bokor, N. Ceglio, K. Jackson, M. Koike, and J. Underwood, "Undulator radiation for at-wavelength interferometry of optics for extreme-ultraviolet lithography," *Appl. Opt.*, vol. 32, pp. 7022–7031, 1993.
- [10] C. Chang, P. Naulleau, E. Anderson, and D. Attwood, "Spatial coherence characterization of undulator radiation," *Opt. Commun.*, vol. 182, pp. 25–34, 2000.
- [11] P. Naulleau, K. Goldberg, P. Batson, J. Bokor, P. Denham, and S. Rekawa, "Fourier-synthesis custom-coherence illuminator for extreme ultraviolet microfield lithography," *Appl. Opt.*, vol. 42, pp. 820–826, 2003.
- [12] J. Taylor, D. Sweeney, R. Hudyma, L. Hale, T. Decker, G. Kubiak, W. Sweatt, and N. Wester, EUV Microexposure Tool (MET) for near-term development using a high NA projection system, presented at Proc. 2nd Int. EUVL Workshop, [Online]. Available: [http://www.semtech.org/resources/litho/meetings/euvl/20001019/707\\_SYS07\\_taylor.pdf](http://www.semtech.org/resources/litho/meetings/euvl/20001019/707_SYS07_taylor.pdf)
- [13] R. Hudyma, J. Taylor, D. Sweeney, L. Hale, W. Sweatt, and N. Wester, "E-D characteristics and aberration sensitivity of the Microexposure Tool (MET)," in *2nd International EUVL Workshop*, Oct. 19–20, 2000.
- [14] P. Naulleau, P. Denham, and S. Rekawa, "Design and implementation of a vacuum-compatible laser-based subnanometer-resolution absolute distance measurement system," *Opt. Eng.*, vol. 44, pp. 1–5, 2005.
- [15] P. Naulleau, P. Denham, B. Hoef, and S. Rekawa, "A design study for synchrotron-based high-numerical-aperture scanning illuminators," *Opt. Comm.*, vol. 234, pp. 53–62, 2004.

- [16] K. Goldberg, P. Naulleau, P. Denham, S. Rekawa, K. Jackson, J. Liddle, and E. Anderson, "EUV interferometric testing and alignment of the 0.3 NA MET optic," *Proc. SPIE*, vol. 5374, pp. 64–73, 2004.
- [17] K. Goldberg, P. Naulleau, P. Denham, S. Rekawa, K. Jackson, E. Anderson, and J. Liddle, "At-wavelength alignment and testing of the 0.3 NA MET optic," *J. Vac. Sci. Technol.*, vol. B 22, pp. 2956–2961, 2004.
- [18] T. Koehler, R. Brainard, P. Naulleau, D. van Steenwinkel, J. Lammers, K. Goldberg, J. Mackevich, and P. Trefonas, "Performance of EUV photoresists on the ALS micro exposure tool," *Proc. SPIE*, vol. 5753, pp. 754–764, 2005.
- [19] P. Naulleau, K. Goldberg, E. Anderson, J. Cain, P. Denham, B. Hoef, K. Jackson, A. Morlens, S. Rekawa, and K. Dean, "EUV microexposures at the ALS using the 0.3-NA MET projection optics," *Proc. SPIE*, vol. 5751, pp. 56–63, 2005.
- [20] J. Cain, P. Naulleau, and C. Spanos, "Lithographic measurement of EUV flare in the 0.3-NA MET optic," *Proc. SPIE*, vol. 5751, pp. 301–311, 2005.
- [21] P. Naulleau, "Verification of point-spread function based modeling of an extreme ultraviolet photoresist," *Appl. Opt.*, vol. 43, pp. 788–792, 2004.
- [22] S. Lee, D. Tichenor, and P. Naulleau, "Lithographic aerial-image contrast measurement in the extreme ultraviolet engineering test stand," *J. Vac. Sci. Technol.*, vol. B 20, pp. 2849–2852, 2002.
- [23] G. M. Wallraff, D. R. Medeiros, M. Sanchez, K. Petrillo, W. Huang, C. Rettner, B. Davis, C. E. Larson, L. Sundberg, P. J. Brock, W. D. Hinsberg, F. A. Houle, J. A. Hoffnagle, D. Goldfarb, K. Temple, S. Wind, and J. Buccignano, "Sub-50 nm half-pitch imaging with a low activation energy chemically amplified photoresist," *J. Vac. Sci. Technol.*, vol. B 22, pp. 3479–3484, 2004.

**Patrick Naulleau** received the B.S. and M.S. degrees in electrical engineering from the Rochester Institute of Technology, Rochester, NY, in 1991 and 1993, respectively, and the Ph.D. in electrical engineering from the University of Michigan, Ann Arbor, in 1997.

From 1997 to 2005, he was a Staff Scientist at Lawrence Berkeley National Laboratory, Berkeley, CA, where he worked at the Center for X-ray Optics in the area of EUV interferometry and lithography. In 2005, Patrick joined the College of Nanoscale Science and Engineering, University at Albany, State University of New York, where he holds the position of Associate Professor. There, he is continuing his research in the areas of advanced lithography and metrology with present concentration on the EUV regime. He has published well over 100 papers in the areas of optics, metrology, and lithography.

**Kenneth A. Goldberg** was born in San Francisco, CA. He received the B.S. degree in physics and applied mathematics and the M.S. and Ph.D. degrees in physics from the University of California at Berkeley in 1992, 1994, and 1997, respectively.

He is a Staff Physicist at the Center for X-Ray Optics at Lawrence Berkeley National Laboratory, Berkeley, CA, working on high-accuracy metrology techniques for short-wavelength, and EUV optical systems. He has worked on the development of EUV lithography technologies, interferometry techniques, synchrotron radiation applications, and optical system modeling since 1993. He holds several patents and has published extensively on short-wavelength interferometry techniques, including point-diffraction and shearing interferometers.

Dr. Goldberg received the UC Berkeley Physics Department Citation in 1992 and the Advanced Light Source Halbach Prize for Instrumentation in 1998. He is a member of OSA and SPIE.

**Jason P. Cain** (M'04) received the B.S. degree in electrical engineering from Texas A&M University, College Station, in 1999 and the M.S. and Ph.D. degrees in electrical engineering and computer sciences from the University of California, Berkeley, in 2002 and 2004, respectively.

He is currently with the Automated Precision Manufacturing Group, Advanced Micro Devices, Sunnyvale, CA, where his research interests include metrology and process control of the lithographic patterning process.

Dr. Cain is a member of SPIE and Eta Kappa Nu.

**Erik H. Anderson** received the B.S. degree in 1981, the M.S. degree in 1984, and the Ph.D. degree in 1988 from the Department of Electrical Engineering and Computer Science, Massachusetts Institute of Technology, Cambridge, MA.

He joined Lawrence Berkeley National Laboratory, Berkeley, CA, in 1988 and worked as a Visiting Scientist at the IBM T.J. Watson Research Laboratory, Yorktown Heights, NY, developing zone plate optics for X-ray microscopy. In 1993, he moved to Berkeley to build and manage the Nanofabrication facility within the Center for X-Ray Optics. In 2001, he became the Director of the Center for X-Ray Optics. He is currently involved in EUV and soft X-ray optics development, characterization, nanofabrication, and X-ray microscopy.

**Kim R. Dean** received the Ph.D. degree in physical chemistry from the University of Texas, Austin, in 1990 for her research in the photophysical properties of polymers.

Currently, she is the Project Manager of the EUV Resist Development Group at SEMATECH, Austin, TX. Prior to that, she worked on development projects for 157-, 193-, and 248-nm photoresists at SEMATECH. She has published over 20 papers in the areas of resist and other topics.

**Paul Denham** entered the Navy after high school where he worked from 1970–1981 as an Electronics Technician Chief and Reactor Operator on nuclear submarines. After the navy, he spent a year working as a Machinist and Engine Technician in an automotive shop.

He then joined Fairchild Semiconductor where he worked from 1983 to 1987 as an Associate Electronics Engineer. Since 1988, Paul has been working for the Center for X-ray Optics at Lawrence Berkeley National Laboratory, Berkeley, CA. He initially worked in the area of multilayer deposition but has since become primarily involved in the design and implementation of nanometer motion control systems, precision in-vacuum manipulation and sensing devices.

**Brian Hoef** received the Associates degree in electronics from City College of San Francisco, San Francisco, CA, in 1997.

He is currently a Mechanical Technologist at the Center for X-ray Optics, Materials Science Division, Lawrence Berkeley National Laboratory, Berkeley, CA, and one of the EUV lithography support team members. His current responsibilities include tool operation and maintenance for the advanced EUV lithography program as well as user support.

**Keith H. Jackson** (M'87) received the Ph.D. degree in physics from Stanford University, Stanford, CA, in 1982.

He is currently the Associate Director of the Center for X-ray Optics, Materials Science Division, Lawrence Berkeley National Laboratory, Berkeley, CA, and one of the EUV lithography team members. His research areas include extreme ultraviolet lithography, synchrotron radiation research, nanoscience and the fabrication of high aspect ratio microstructures using deep etch X-ray lithography. His current scientific research interest focuses on imaging studies of EUV resists and masks. He has authored and coauthored more than 30 papers in international scientific journals.

Dr. Jackson serves as the current President of the National Society of Black Physicists.